

Electron topological transitions of $3\frac{1}{2}$ kind in metals

G.P. Mikitik · Yu.V. Sharlai

Received: 26.06.2015 / Accepted: date

Abstract We consider electron topological transitions associated with certain points of band-contact lines in metals. These transitions are $3\frac{1}{2}$ kind according to the classification of Lifshits and are widespread in metals with inversion symmetry and a weak spin-orbit interaction. The $3\frac{1}{2}$ -order transitions can be detected with the magnetic susceptibility. As an example, we consider these transitions in graphite.

Keywords electron topological transition · band-contact line · magnetic susceptibility · graphite

PACS 71.30.+h · 71.18.+y

1 Introduction

At electron topological transitions of $2\frac{1}{2}$ kind a pocket of the Fermi surface (FS) appears (disappears), or a neck of the FS forms (disrupts) [1–4]. These transitions occur at the critical points \mathbf{p}_c in the Brillouin zone at which the electron energy ε has an extremum or a saddle point in its dependence on the quasi-momentum \mathbf{p} . A small vicinity of such a point gives the singular (nonanalytic) contribution $\delta v(\varepsilon_F)$ to the electron density of states $v(\varepsilon_F)$, $\delta v \propto (\varepsilon_F - \varepsilon_c)^{1/2}$, where ε_F is the Fermi energy of the metal, and $\varepsilon_c = \varepsilon(\mathbf{p}_c)$ is the critical energy. It is also known [2] that if a contact line of two electron energy bands exists in the Brillouin zone, the Fermi surface can have a self-intersecting shape, and the points of the line at which such surfaces appear or disappear correspond to electron topological transitions, too. At these points in the band-contact lines the common energy of the two touching bands reaches its maximum or minimum. In this paper we discuss the topological transitions associated with the appearance (disappearance) of self-intersecting Fermi surfaces in metals [5]. It turns out that these transitions are $3\frac{1}{2}$ kind according to the classification

G.P. Mikitik · Yu.V. Sharlai

B. Verkin Institute for Low Temperature Physics & Engineering, Ukrainian Academy of Sciences,
Kharkov 61103, Ukraine.

of Lifshits [1]. We also point out how these transitions can be detected in experiments. As an example, we consider the transitions in graphite.

2 Electron topological transitions

It is common knowledge that the contact of the electron energy bands in a metal can occur at symmetry points and along symmetry axis of its Brillouin zone. Besides, as was shown by Herring [6], there are lines of an *accidental* contact between two bands in crystals. The term "accidental" means that the degeneracy of electron states is not caused by their symmetry. Such band-contact lines are widespread in metals with inversion symmetry and with a weak spin-orbit interaction. This follows from one of Herring's results [6]: if there is a point of an intersection of two energy bands in an axis of symmetry of the Brillouin zone, a band-contact line perpendicular to the axis has to pass through this point. Intersection of the bands at points in the axes frequently occurs even in simple metals [7]. The literature data show that the lines of the accidental contact exist, for example, in Be, Mg, Zn, Cd, Al, and many other metals. Besides, the band-contact lines occur in graphite [8–10], rhombohedral multilayer graphene [11, 12], three dimensional graphene networks [13], and in bcc Fe [14]. These lines (called the Dirac line nodes) exist also in the topological line-node semimetals Ca_3P_2 [15] and Cu_3NPd [16, 17]. In experiments, the band-contact lines in metals can be, in principle, detected via the phase analysis of the de Haas-van Alphen (or Shubnikov-de Haas) oscillations since the phase of these oscillations is determined by the number of the band-contact lines penetrating the appropriate cross-section of the Fermi surface [18–20].

The band-contact lines are either closed curves in the Brillouin zone or end on the surfaces of this zone. In both the cases the energy of the two touching bands in the degeneracy line is a periodic function of the quasi-momentum running this line, and the energy of the bands changes between its minimum ε_{min} and maximum ε_{max} values. At this ε_{min} the self-intersecting FS necessarily appears and at ε_{max} it disappears. Thus, these electron topological transitions are widespread in metals no less than the $2\frac{1}{2}$ -order transitions of Lifshits.

Consider the point \mathbf{p}_c in a contact line of the bands 1 and 2 at which the common energy of the two bands reaches its extremum ε_c . The spectrum of these two bands near this critical point can be always represented in the form [5]:

$$\varepsilon_{1,2}(\mathbf{p}) = \varepsilon_c + Bp_z^2 + \mathbf{v}_\perp \cdot \mathbf{p}_\perp \pm [b_{xx}p_x^2 + b_{yy}p_y^2]^{1/2}, \quad (1)$$

where the quasi-momentum \mathbf{p} is measured from \mathbf{p}_c , $\mathbf{p}_\perp = (p_x, p_y)$, the p_z axis is along the tangent to the band-contact line at the point \mathbf{p}_c , and constants B , $\mathbf{v}_\perp = (v_x, v_y)$, $b_{xx} > 0$, $b_{yy} > 0$ are the parameters of the spectrum. The parameter B is positive if $\varepsilon_c = \varepsilon_{min}$, and $B < 0$ if $\varepsilon_c = \varepsilon_{max}$. As shown in Ref. [5], the shape of the self-intersecting surfaces essentially depends on the only parameter,

$$\tilde{a}^2 \equiv \frac{v_x^2}{b_{xx}} + \frac{v_y^2}{b_{yy}}. \quad (2)$$

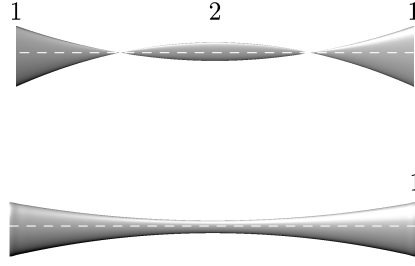


Fig. 1 The Fermi surfaces near $\varepsilon_c = \varepsilon_{min}$ at $\tilde{a}^2 < 1$. Bottom: $\varepsilon_F < \varepsilon_{min}$. Top: $\varepsilon_F > \varepsilon_{min}$. The band-contact line is shown by the dash line. The numbers 1 and 2 mark the Fermi surfaces corresponding to the bands 1 and 2.

If $\tilde{a}^2 < 1$ and the difference $\varepsilon_F - \varepsilon_c$ changes, the appearance of the self-intersecting Fermi surface occurs in the manner shown in Fig. 1. This topological transition can be considered as a combination of the two transitions, viz. the Fermi-surface neck of the band 1 disrupts, and simultaneously a new pocket of the band 2 appears. In the case $\tilde{a}^2 > 1$, although the self-intersecting Fermi surface appears or disappears when ε_F crosses ε_c , its topological properties do not change at this crossing [5]. In other words, the electron topological transition occurs only at $\tilde{a}^2 < 1$.

Near $\varepsilon_F = \varepsilon_c$ the density of the electron states $\nu(\varepsilon_F)$ calculated per unit volume of the crystal is the sum of its regular part $\nu_{reg}(\varepsilon_F)$ and of its singular part $\delta\nu(\varepsilon_F)$. The latter is due to the electron topological transition and differs from zero when $\Delta\varepsilon_F \equiv (\varepsilon_F - \varepsilon_c)\text{sgn}(B) > 0$. This singular $\delta\nu(\varepsilon_F)$ exists only if $\tilde{a}^2 < 1$,

$$\delta\nu(\varepsilon_F) = \frac{4(\Delta\varepsilon_F)^{3/2}}{3\pi^2\hbar^3|B|^{1/2}(1-\tilde{a}^2)^{3/2}(b_{xx}b_{yy})^{1/2}}, \quad (3)$$

where we have taken into account the double degeneracy of the electron states in spin. If $\tilde{a}^2 > 1$, the singular term is absent. It follows from formula (3) that the topological transitions considered here are the $3\frac{1}{2}$ -order transitions according to the classification of Lifshits [1,2]. Note also that the singularity in the density of the electron states, $\delta\nu \propto (\varepsilon_F - \varepsilon_c)^{3/2}$, is weaker than the singularity $\delta\nu \propto (\varepsilon_F - \varepsilon_c)^{1/2}$ at the well-known topological transitions of $2\frac{1}{2}$ kind [1–4]. This change of the singularity, e.g., at the appearance of the pocket in Fig. 1 is due to the following: The transverse dimensions of the new Fermi-surface pocket of the band 2 are proportional to $\Delta\varepsilon_F$ and hence are small as compared to its longitudinal dimension that is proportional to $(\Delta\varepsilon_F)^{1/2}$. Then, one has $\delta N \propto (\Delta\varepsilon_F)^{5/2}$ for the number of the electrons in the pocket and $\delta\nu \propto (\Delta\varepsilon_F)^{3/2}$. On the other hand, in the case of the appearance of a Fermi-surface pocket at the electron topological transition of $2\frac{1}{2}$ kind, all its dimensions are of the order of $(\Delta\varepsilon_F)^{1/2}$, $\delta N \propto (\Delta\varepsilon_F)^{3/2}$, and $\delta\nu \propto (\Delta\varepsilon_F)^{1/2}$.

At the topological transitions of the $3\frac{1}{2}$ kind the singularities of the physical quantities that are proportional to the density of the electron states ν or its derivative $d\nu/d\varepsilon_F$ are weaker than the singularities at the topological transitions of the $2\frac{1}{2}$ kind. This makes a detection of the $3\frac{1}{2}$ -order transitions difficult with measurements of these quantities. However, these transitions can be detected with the mag-

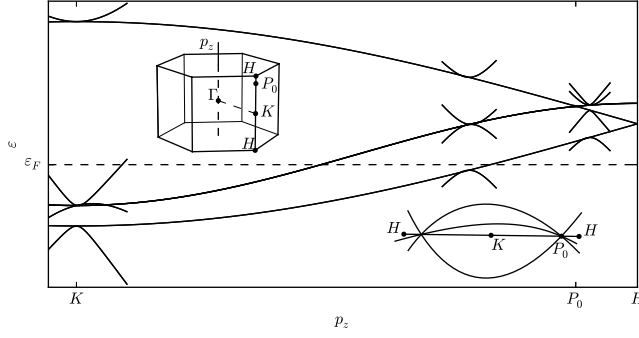


Fig. 2 The schematic representation of the dependences of the electron energy bands ε_i ($i = 1 - 4$) in graphite on the quasi-momentum \mathbf{p} near the edge HKH of its Brillouin zone. Shown are the dependences $\varepsilon_i(p_z)$ at $p_\perp = 0$ and the dependences of ε_i on $p_\perp = \sqrt{p_x^2 + p_y^2}$ at some characteristic values of p_z according to the model [23]. The dashed line marks the position of the Fermi level ε_F . The top insert shows the Brillouin zone of graphite and its characteristic points. The lower insert schematically shows the four contact lines of the bands $\varepsilon_2(\mathbf{p})$ and $\varepsilon_3(\mathbf{p})$ in the vicinity of the edge HKH.

netic susceptibility since its orbital part generally is not determined by the density of the electron states, and at the $3\frac{1}{2}$ -order transitions the component χ_{zz} of the magnetic-susceptibility tensor exhibits a giant diamagnetic anomaly [21]. At low temperatures $T \ll \Delta\varepsilon_F \equiv (\varepsilon_F - \varepsilon_c)\text{sgn}(B)$ and weak magnetic fields H , one has for $\Delta\varepsilon_F > 0$ [21]

$$\chi_{zz}(\varepsilon_F) = -\frac{e^2}{6\pi^2 c^2 \hbar} \left(\frac{b_{xx} b_{yy}}{|B|} \right)^{1/2} \frac{(1 - \tilde{a}^2)^{3/2}}{(\Delta\varepsilon_F)^{1/2}}. \quad (4)$$

Thus, the anomaly is the large peak in the ε_F -dependence of $|\chi_{zz}|$. Interestingly, the singularity in the susceptibility, $\chi_{zz}(\varepsilon_F) \propto (\Delta\varepsilon_F)^{-1/2}$, is the same as the singularity in the thermoelectric power at the $2\frac{1}{2}$ -order transitions [3]. The divergence of expression (4) for $\Delta\varepsilon_F \rightarrow 0$ should be cut off at $\Delta\varepsilon_F \sim T$, and this cut-off determines the magnitude $|\chi_{zz}|_{\max} \propto T^{-1/2}$ of the diamagnetic peak at weak magnetic fields. With increasing magnetic field, the energy spacing $\Delta\varepsilon_H \propto H^{1/2}$ between the Landau levels begins to exceed the temperature. In this case the magnitude of the diamagnetic peak is determined by this spacing, and we have $|\chi_{zz}|_{\max} \propto (\Delta\varepsilon_H)^{-1/2} \propto H^{-1/4}$ [22].

3 Graphite

Figure 2 shows the Brillouin zone of graphite and its four electron energy bands $\varepsilon_i(\mathbf{p})$ ($i = 1 - 4$) near the edge H-K-H of this zone. These bands are described by the model of Ref. [23], and parameters of this model were found from the analysis of various experimental data [24]. We use these parameters in all the calculations below. The line P_0 -K- P_0 is the contact line of the bands $\varepsilon_2(\mathbf{p})$ and $\varepsilon_3(\mathbf{p})$. Besides, near this line there are three additional lines of the accidental contact of the same bands [8,9], see Fig. 2. These additional lines cross the plane $p_z = 0$ at the small

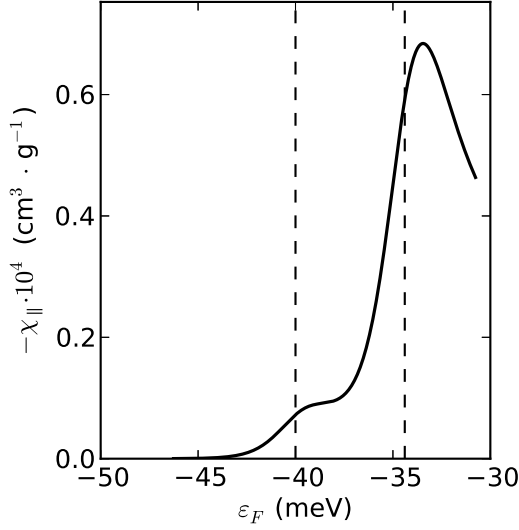


Fig. 3 Dependence of the specific magnetic susceptibility χ_{\parallel} of graphite on the position of the Fermi level ε_F at temperature $T = 10$ K. The dashed lines mark the critical energies ε_c for the central and side band-contact lines.

distance $p_{\perp}^0 = 0.0554(\hbar/a_0)$ from the point K. Here $a_0 = 2.461 \cdot 10^{-8}$ cm is the in-plane lattice parameter of graphite.

For the central band-contact line P₀-K-P₀, the minimum ε_c of the common energy of the two bands is reached at the point K (i.e., at $p_z = 0$), $\varepsilon_c = -40$ meV, and the parameters of the spectrum (1) are the following: $v_x = v_y = 0$, $B = \tilde{B}(c_0/\hbar)^2$, $b_{xx} = b_{yy} = \tilde{b}(a_0/\hbar)^2$ where $\tilde{B} = 10$ meV, $\tilde{b} = 0.2992$ eV², and $c_0 = 6.708 \cdot 10^{-8}$ cm is the lattice parameter along the z axis of graphite. For the side band-contact lines, the minimum ε_c of the common energy of the bands $\varepsilon_2(\mathbf{p})$ and $\varepsilon_3(\mathbf{p})$ is reached at $p_z = 0$, $p_{\perp} = p_{\perp}^0$. At these points $\varepsilon_c = -34.4$ meV, and the parameters of the spectrum (1) are $v_x = \tilde{v}_x(a_0/\hbar)$, $v_y = 0$, $B = \tilde{B}(c_0/\hbar)^2$, $b_{xx} = \tilde{b}_{xx}(a_0/\hbar)^2$, $b_{yy} = \tilde{b}_{yy}(a_0/\hbar)^2$ where the p_x axis is along the direction $K\Gamma$, $\tilde{v}_x = 0.1957$ eV, $\tilde{B} = 7.2$ meV, $\tilde{b}_{xx} = 0.2744$ eV², and $\tilde{b}_{yy} = 2.4809$ eV².

With these parameters of the band-contact lines, we calculate the dependence of the specific magnetic susceptibility χ_{\parallel} of graphite along the z axis on the position of the Fermi level ε_F , Fig. 3. In the calculation of χ_{\parallel} we use formula (4) generalized to the case of finite temperature [21], the density of graphite $\rho = 2.2$ g/cm³, and we take into account that there are two points K and 6 side critical points in the Brillouin zone. Formula (4) gives only the susceptibility of the electron states near the critical points in the band-contact lines. All other electron states produce a practically constant contribution to χ_{\parallel} , and we omit this contribution here. The data shown in Fig. 3 are valid in weak magnetic fields when $\Delta\varepsilon_H < T < 3.6$ meV. The value 3.6 meV is the height of the energy barrier separating the ε_c for the side band-contact lines from the ε_c of the central line. When the distance between the Landau levels $\Delta\varepsilon_H$ exceeds this value, the critical points of the band-contact lines cannot be considered

separately, and $\chi_{||}$ will change. If $T = 10$ K, the criterion of weak magnetic fields, $\Delta\varepsilon_H < T$, holds at $H < 130$ Oe since $\Delta\varepsilon_H \sim 0.88\sqrt{H[\text{Oe}]}$ K for the central critical point.

Finally, we note that the $3\frac{1}{2}$ -order topological transition in beryllium was theoretically investigated in Ref. [25].

4 Conclusions

We have theoretically studied the electron topological transitions of the $3\frac{1}{2}$ kind associated with band-contact lines in metals. These transitions can be detected with measurements of the magnetic susceptibility. As an example, we have presented the magnetic susceptibility calculated near electron topological transitions of the $3\frac{1}{2}$ kind in graphite.

References

1. I.M. Lifshits, Zh. Eksp. Teor. Fiz. **38**, 1569 (1960) [Sov. Phys. JETP **11**, 1130 (1960)].
2. I.M. Lifshits, M. Ya. Azbel', and M.I. Kaganov, *Electron Theory of Metals* (Consultants Bureau, New York, 1973).
3. A.A. Varlamov, V.S. Egorov, A.V. Pantsulaya, Advances in Physics **38**, 469 (1989).
4. Ya.M. Blanter, M.I. Kaganov, A.V. Pantsulaya, A.A. Varlamov, Physics Reports **245**, 159 (1994).
5. G.P. Mikitik, Yu.V. Sharlai, Phys. Rev. B **90**, 155122 (2014).
6. C. Herring, Phys. Rev. **52**, 365 (1937).
7. D. A. Papaconstantopoulos, *Handbook of the Band Structure of Elemental Solids* (Plenum, New York, 1986).
8. G.P. Mikitik, Yu.V. Sharlai, Phys. Rev. B **73**, 235112 (2006).
9. G.P. Mikitik, Yu.V. Sharlai, Fiz. Nizk. Temp. **34**, 1012 (2008) [Low Temp. Phys. **34**, 794 (2008)].
10. T.T. Heikkilä and G.E. Volovik, New J. Phys. **17**, 093019 (2015).
11. T.T. Heikkilä and G.E. Volovik, JETP Lett. **93**, 59 (2011).
12. D. Pierucci, H. Sediri, M. Hajlaoui, J.-C. Girard, T. Brumme, M. Calandra, E. Velez-Fort, G. Patriarce, M.G. Silly, G. Ferro, V. Soulière, M. Marangolo, F. Sirotti, F. Mauri, and A. Ouerghi, ACS Nano **9**, 5432 (2015).
13. H. Weng, Y. Liang, Q. Xu, R. Yu, Z. Fang, X. Dai, Y. Kawazoe, Phys. Rev. B **92**, 045108 (2015).
14. D. Gosálbez-Martínez, I. Souza, and D. Vanderbilt, Phys. Rev. B **92**, 085138 (2015).
15. L. S. Xie, L. M. Schoop, E. M. Seibel, Q. D. Gibson, W. Xie, and R. J. Cava, APL Mater. **3**, 083602 (2015).
16. Y. Kim, B.J. Wieder, C. L. Kane and A.M. Rappe, Phys. Rev. Lett. **115**, 036806 (2015).
17. R. Yu, H. Weng, Z. Fang, X. Dai, X. Hu, Phys. Rev. Lett. **115**, 036807 (2015).
18. G.P. Mikitik, Yu.V. Sharlai, Zh. Eksp. Teor. Fiz. **114**, 1375 (1998) [JETP **87**, 747 (1998)].
19. G.P. Mikitik, Yu.V. Sharlai, Phys. Rev. Lett. **82**, 2147 (1999).
20. G.P. Mikitik, Yu.V. Sharlai, Fiz. Nizk. Temp. **33**, 586 (2007) [Low Temp. Phys. **33**, 439 (2007)].
21. G.P. Mikitik, I.V. Svechkarev, Fiz. Nizk. Temp. **15**, 295 (1989) [Sov. J. Low Temp. Phys. **15**, 165 (1989)].
22. G.P. Mikitik, Yu.V. Sharlai, Fiz. Nizk. Temp. **22**, 762 (1996) [Low Temp. Phys. **22**, 585 (1996)].
23. J.C. Slonczewski, P.R. Weiss, Phys. Rev. **109**, 272 (1958).
24. N.B. Brandt, S.M. Chudinov, and Ya.G. Ponomarev, *Semimetals I. Graphite and its Compounds* (Elsevier, Amsterdam, 1988).
25. G.P. Mikitik, Yu.V. Sharlai, Fiz. Nizk. Temp. **41**, 1276 (2015) [Low Temp. Phys. **41**, 996 (2015)].